

# Hierarchical Full-Duplex Underwater Acoustic Network: A NOMA Approach

Esraa A. Makled<sup>1</sup>, Animesh Yadav<sup>1</sup>, Octavia A. Dobre<sup>1</sup> and Ronald D. Haynes<sup>2</sup>  
<sup>1</sup>Faculty of Engineering and Applied Sciences, <sup>2</sup>Department of Mathematics and Statistics

Memorial University, St. John's, Canada

Email: {eamakled, animeshy, odobre, and rhaynes}@mun.ca

**Abstract**—Underwater acoustic is the prevalent technology in underwater wireless communications. The sum rate in underwater acoustic channels is limited by the underwater environment properties. This paper attempts to increase the sum rate of underwater channels without utilizing additional resources, through adding a relay and employing full duplex (FD) and non-orthogonal multiple access (NOMA) technologies. The adopted system model has two sensors and two robotic arms communicating with a buoy via a relay. Employing FD-NOMA allows multiple uplink and downlink transmissions to occur simultaneously, using the same time and frequency resources. The main challenge for this deployment is the interference between the transmissions. Interference cancellation techniques, successive interference cancellation and self-interference cancellation, are employed to mitigate the interference due to NOMA and FD, respectively. In order to maximize the sum rate, an optimization problem over the power is formulated and solved as a convex optimization problem. The performance of the system is benchmarked with the performance of the non-relay (NR) aided FD-NOMA and relay-aided (R) half duplex orthogonal multiple access (HD-NOMA). It is shown that R-FD-NOMA always has higher sum rate than NR-FD-NOMA, irrespective of the efficiency of interference cancellation. In addition, it is shown that at efficient interference cancellation, the sum rate of FD-NOMA is higher than HD-NOMA.

**Index Terms**—Underwater wireless communications, underwater acoustic communications, full duplex (FD), non-orthogonal multiple access (NOMA), and convex optimization.

## I. INTRODUCTION

Oceanic applications, such as oil and gas exploration and pipeline monitoring, rely on underwater wireless communications [1]–[3]. The common examples of under water wireless communication technologies are acoustic, optical wireless and radio frequency communication. The long-range wireless communications is dominated by underwater acoustic (UWA) transmission [2]. UWA communication is challenging due to the complex underwater environment, where signals suffer from multiple reflections, severe dispersions and variations. Besides, the UWA channel is characterized by long propagation delay due to the slow acoustic wave speed [1]. These characteristics limit the sum rate of UWA channels.

In addition, underwater devices are power limited. Hence, relays are used to increase the power utilization efficiency, channel reliability and transmission distance. Incorporating relays supports the communication systems by amplifying and forwarding or decoding and forwarding the data, among other strategies [4]–[6].

Furthermore, technologies such as full duplex (FD) and non-orthogonal multiple access (NOMA) are indispensable for enhancing the sum rate without additional radio resources. FD communications enhance the channel rate by allowing for simultaneous transmission and reception of signals on the same frequency. Owing to the self-interference (SI) caused by the FD operation, the rate enhancement is possible only if the SI is cancelled up to the noise level. Theoretically, FD can double the throughput of the system when compared to the conventional half duplex [7]. On the other hand, NOMA allows the multiplexing of multiple users at the same time and frequency resource, and hence, improves the rate [8]. NOMA differentiates between users by assigning different power levels (power-domain NOMA) or different codes (code-domain NOMA). The power level assignment depends on the channel strength. NOMA was shown to provide better spectral efficiency than orthogonal multiple access (OMA) systems in wireless communications [8].

Previously, FD and NOMA have been investigated independently in UWA communications [9], [10]. In this paper, FD and NOMA are integrated with a relay-based UWA network with the goal of improving the network sum rate and reliability. The integration of FD and NOMA is not straightforward, especially in underwater channels and with the additional interferences in uplink (UL) and downlink (DL) channels, and SI. A sum rate maximization problem is formulated for UWA channels under interference and transmission power constraints. The problem is solved by optimizing the transmission powers to provide the highest sum rate.

The rest of this paper is organized as follows: Section II describes the system model, Section III formulates the sum rate maximization problem and Section IV presents the solution for the problem. The results are shown in Section IV and Section V concludes the paper.

## II. SYSTEM MODEL

Consider a hierarchical UWA communication system consisting of an FD-buoy (B), an FD-relay (R), two sensors ( $S_1$  and  $S_2$ ) and two robotic actuators ( $RA_1$  and  $RA_2$ ), as depicted in Fig. 1. The sensors send data to the buoy on the UL channel, while the buoy sends data to the two RAs on the DL channels. Both UL and DL channels use the relay node, which decodes-and-forwards the received data to the buoy and RAs, respectively.

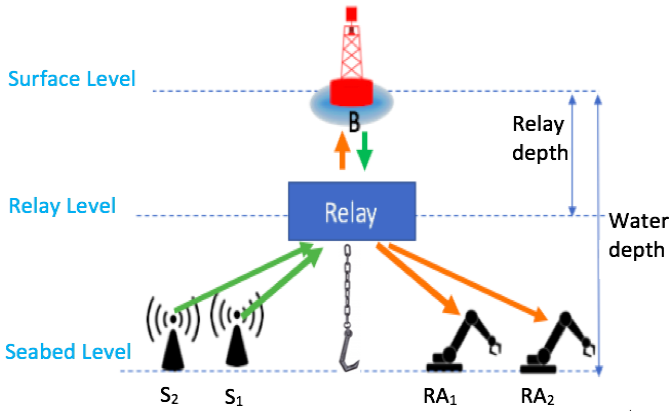


Fig. 1: System model.

The channels  $B \rightarrow R$ ,  $S_1 \rightarrow R$  and  $S_2 \rightarrow R$  form the UL-NOMA group, whereas  $R \rightarrow B$ ,  $R \rightarrow RA_1$  and  $R \rightarrow RA_2$  form the DL-NOMA group. In NOMA, the receiver performs successive interference cancellation (SuIC) on strong interfering signals in order to guarantee accurate signal detection. The SuIC efficiency is represented by  $\theta \in [0, 1]$ , where  $\theta = 0$  denotes perfect SuIC.

The relay and buoy employ SI cancellation (SIC) techniques and are left with residual SI (RSI), which is presented by  $I_A$  as:

$$I_A = \frac{p_A^{(1-\lambda)}}{\beta \mu^\lambda}, \quad (1)$$

where  $A \in \{R, B\}$ ,  $p_A$  denotes the transmission power of the relay or buoy,  $\beta$  is the interference suppression factor due to passive cancellation technique, and  $\mu$  and  $\lambda$  are SIC cancellation factors [7], [11]. In order to study the impact of imperfect SIC on the system performance,  $\lambda$  is varied between 0 and 1 as per [11], where  $\lambda = 0$  and 1 correspond to no and perfect SIC, respectively.

The UWA channel is usually characterized by slow propagation and the distinct reflections of the signal from the sea bottom and surface. Consequently, signals are delayed differently at the receiver. For the UWA channel gain,  $G$ , there is no standard statistical channel model available. We chose the model that includes large- and small-scale fading in [12], as

$$G = \mathbb{E} \left\{ \frac{1}{W} \int_{f_0}^{f_0+W} |\bar{H}_0(f) \sum_{\ell} h_{\ell} \tilde{\gamma}_{\ell}(f, t) e^{-2\pi f_{\ell} \tau_{\ell}}|^2 df \right\}, \quad (2)$$

where  $\bar{H}_0$  represents the channel filtering effect, and  $h_{\ell}$  and  $\tau_{\ell}$  are large-scale parameters on the  $\ell$ th path. The small-scale fading effect on the channel is represented by  $\gamma_{\ell}(f, t) e^{2\pi a_{\ell} f t}$ .  $\gamma_{\ell}$  is the small-scale fading coefficient, while  $a_{\ell}$  is the Doppler scaling factor on the  $\ell$ th path.  $W$  is the bandwidth and  $f_0$  is the minimum frequency of the channel.

Next, for each channel, the signal-to-interference-plus-noise ratios (SINRs) for the channels  $S_1 \rightarrow R$ ,  $S_2 \rightarrow R$ ,  $B \rightarrow R$ ,  $R \rightarrow RA_1$ ,  $R \rightarrow RA_2$  and  $R \rightarrow B$ , are respectively defined as:

$$\gamma_1(\mathbf{p}) = \frac{p_{S_1} G_{S_1,R}}{p_{S_2} G_{S_2,R} + \theta p_B G_{B,R} + I_R + \sigma_N^2} \quad (3)$$

$$\gamma_2(\mathbf{p}) = \frac{p_{S_2} G_{S_2,R}}{\theta p_{S_1} G_{S_1,R} + \theta p_B G_{B,R} + I_R + \sigma_N^2}, \quad (4)$$

$$\gamma_3(\mathbf{p}) = \frac{p_B G_{B,R}}{p_{S_1} G_{S_1,R} + p_{S_2} G_{S_2,R} + I_R + \sigma_N^2}, \quad (5)$$

$$\gamma_4(\mathbf{p}) = \frac{p_{R_1} G_{R,RA_1}}{G_{R,RA_1} \sum_{j=2,3} p_{R_j} \omega_j + \sum_{k=1,2,B} p_{S_k} G_{S_k,RA_1} + \sigma_N^2}, \quad (6)$$

$$\gamma_5(\mathbf{p}) = \frac{p_{R_2} G_{R,RA_2}}{G_{R,RA_2} \sum_{j=1,3} p_{R_j} + \sum_{k=1,2,B} p_{S_k} G_{S_k,RA_2} + \sigma_N^2}, \quad (7)$$

$$\gamma_6(\mathbf{p}) = \frac{p_{R_3} G_{R,B}}{\theta G_{R,B} \sum_{j=1,2} p_{R_j} + p_{S_2} G_{S_2,B} + p_{S_1} G_{S_1,B} + I_B + \sigma_N^2}, \quad (8)$$

where  $G_{x,y}$  is the average channel gain on  $x \rightarrow y$ .  $p_{S_1}$ ,  $p_{S_2}$  and  $p_B$  are the transmission powers of  $S_1$ ,  $S_2$ , and  $B$ , respectively.  $p_{R_1}$ ,  $p_{R_2}$ , and  $p_{R_3}$  are the transmission powers from  $R$  to  $RA_1$ ,  $RA_2$ , and  $B$ , respectively. The vector  $\mathbf{p}$  collects  $p_{S_1}$ ,  $p_{S_2}$ ,  $p_B$ ,  $p_{R_1}$ ,  $p_{R_2}$  and  $p_{R_3}$ .  $I_B$  and  $I_R$  are the RSI at  $B$  and  $R$ , respectively. Distances are chosen so that UL channel gains are sorted as  $G_{B,R} > G_{S_1,R} > G_{S_2,R}$ , and the DL channel gains are sorted as  $G_{R,B} > G_{R,RA_1} > G_{R,RA_2}$ .  $\omega_2$  is equal to  $\theta$ , while  $\omega_3$  is equal to 1.

The ambient noise power,  $\sigma_N^2$ , has four components: turbulence noise, shipping noise, wave noise, and thermal noise. The following empirical formulas give the individual power spectral densities (PSDs) of these noise components in dB re  $\mu$  Pa per Hz as a function of frequency  $f$  in kHz [13]:

$$\begin{aligned} N_t(f) &= 17 - 30 \log f, \\ N_s(f) &= 40 + 20(s - 0.5) + 26 \log f - 60 \log(f + 0.03), \\ N_w(f) &= 50 + 7.5w^{1/2} + 20 \log f - 40 \log(f + 0.4), \\ N_{th}(f) &= -15 + 20 \log f. \end{aligned} \quad (9)$$

The shipping activity is represented by  $s \in [0, 1]$ , depending on the level of activity.  $w$  denotes the wind speed in m/s. The overall acoustic PSD is calculated as [13]:

$$N_a(f) = 10^{N_t(f)/10} + 10^{N_s(f)/10} + 10^{N_w(f)/10} + 10^{N_{th}(f)/10}. \quad (10)$$

In order to convert the PSD from acoustic to electrical domain (W/Hz), the following formula is used [4]:

$$N(f) = \frac{10^{-17.2} N_a(f)}{\phi}, \quad (11)$$

where  $N(f)$  is the equivalent electrical noise PSD and  $\phi$  denotes the efficiency of the electric circuit in converting the acoustic power to electrical power.

### III. SUM RATE OPTIMIZATION

In this section, we formulate the sum rate maximization problem using equations (3)-(8), where the relationship between the rate ( $C$ ) and the SINR ( $\gamma$ ) of a channel is expressed as  $C = \log_2(1+\gamma)$  in bps/Hz. The goal is to obtain the optimal transmit powers of the sensors, buoy, and relay nodes. The optimization problem is thus expressed as:

$$\begin{aligned} \max_{\mathbf{p}} \quad & \sum_{i=1}^6 \log_2(1 + \gamma_i(\mathbf{p})) & (12a) \\ \text{s.t.} \quad & C_{\min} \leq C_{S_1,R}, C_{\min} \leq C_{S_2,R}, \\ & C_{\min} \leq C_{RA_1,R}, C_{\min} \leq C_{RA_2,R}, & (12b) \\ & C_{RA_2,R} + C_{RA_2,R} \leq C_{B,R}, & (12c) \\ & C_{S_1,R} + C_{S_2,R} \leq C_{R,B}, & (12d) \\ & p_{R_1} + p_{R_2} + p_{R_3} \leq \bar{p}_R, & (12e) \\ & 0 \leq p_{S_1} \leq \bar{p}_{S_1}, 0 \leq p_{S_2} \leq \bar{p}_{S_2}, 0 \leq p_B \leq \bar{p}_B, \\ & 0 \leq p_{R_1}, 0 \leq p_{R_2}, 0 \leq p_{R_3}, & (12f) \end{aligned}$$

where  $\bar{p}_{S_1}$ ,  $\bar{p}_{S_2}$ ,  $\bar{p}_B$ , and  $\bar{p}_R$  denote the maximum transmit powers of  $S_1$ ,  $S_2$ ,  $B$ , and  $R$ , respectively.  $C_{x,y}$  represents the rate of channel  $x \rightarrow y$ . The constraints in (12b) guarantee that every channel gets a minimum rate of  $C_{\min}$ . Constraints (12c) and (12d) limit the sum rates of DL channels,  $C_{R,RA_1}$  and  $C_{R,RA_2}$ , and the sum rates of UL channels  $C_{S,RA_1}$  and  $C_{S,RA_2}$  to the achievable capacities of channels,  $C_{R,B}$  and  $C_{B,R}$ , respectively. Furthermore, constraints (12e) and (12f) limit the transmission power of the nodes.

### IV. PROPOSED SOLUTION

It can be observed that (12) is non-convex in nature due to the non-convexity involved in the objective function (12a) and the constraints (12c) and (12d).

Equations (12a), (12c), and (12d) are non-convex because  $\gamma_i(\mathbf{p})$  is a fraction of two functions in  $\mathbf{p}$ . Since the division does not conserve linearity,  $\gamma_i(\mathbf{p})$  is not linear. As a result,  $\log_2(1+\gamma_i(\mathbf{p}))$  is neither concave nor convex and solving this problem optimally is computationally challenging especially for UWA devices. To solve (12) more efficiently, we transform (12) for tractability, approximate the resulting problem by a convex problem, and then propose a rapidly converging iterative algorithm.

To transform the problem into an equivalent problem, we introduce two new slack variables  $x_i$  and  $z_i$  such that:

$$\gamma_i(\mathbf{p}) \triangleq \frac{g_i(\mathbf{p})}{h_i(\mathbf{p})} \geq x_i \quad \forall i, \quad (13)$$

$$x_i z_i \leq g_i(\mathbf{p}) \quad \forall i. \quad (14)$$

$$h_i(\mathbf{p}) \leq z_i \quad \forall i, \quad (15)$$

After applying the transformation, (12) can be equivalently rewritten as:

$$\max_{\mathbf{p}, z_i, x_i} \quad \sum_{i=1}^6 \log_2(1 + x_i) \quad (16a)$$

$$\text{s.t.} \quad x_i z_i \leq g_i(\mathbf{p}) \quad \forall i, \quad (16b)$$

$$h_i(\mathbf{p}) \leq z_i \quad \forall i, \quad (16c)$$

$$(12b) - (12f). \quad (16d)$$

The equivalence between (12) and (16) can be verified by the fact that the newly introduced constraints are active at optimality. It can be observed that (16) is still not convex because of constraints, (16b) and (16c), which are non-convex.

The constraint in equation (16b) is neither convex nor concave because it involves the multiplication of two variables,  $x_i z_i$ . The inequality in (16c) is not convex for all  $i$ . As observed,  $h_i(\mathbf{p})$  in (3)-(5) and (8), have concave interference terms. Given that  $h_i(\mathbf{p})$  is on the left hand side (lesser side) of the inequality, whenever  $h_i(\mathbf{p})$  has interference terms, the constraint in (16c) is not convex. In the following, we approximate these constraints to become convex.

For constraint (16b), we use the upper bound approximation as used in [14] as follows:

$$f(x_i, z_i) = x_i z_i \leq F(x_i, z_i, \xi_i) \triangleq \frac{1}{2\xi_i} x_i^2 + \frac{\xi_i}{2} z_i^2 \quad \forall \xi_i > 0. \quad (17)$$

For  $\hat{\xi}_i = x_i/z_i$ , it can be easily observed that,  $f(x_i, z_i) = F(x_i, z_i, \hat{\xi}_i)$  and  $\nabla f(x_i, z_i) = \nabla F(x_i, z_i, \hat{\xi}_i)$ , where  $\nabla f$  denotes the gradient of  $f$ .

While, for constraint (16c) we approximate  $p^{(1-\lambda)}$ , for  $0 \leq \lambda \leq 1$ , with a first-order Taylor series at  $p(n)$  as follows [15]:

$$\begin{aligned} I_{R_L}(n+1) &= \frac{(p_R(n))^{(1-\lambda)}}{\beta\mu^\lambda} + (1-\lambda) \frac{(p_R(n))^{(-\lambda)}}{\beta\mu^\lambda} \\ &\quad \times (p_R - p_R(n)), \\ I_{B_L}(n+1) &= \frac{(p_B(n))^{(1-\lambda)}}{\beta\mu^\lambda} + (1-\lambda) \frac{(p_B(n))^{(-\lambda)}}{\beta\mu^\lambda} \\ &\quad \times (p_B - p_B(n)), \end{aligned} \quad (18)$$

where  $n$  is the iteration index for Algorithm 1 and  $p_R(n) = \sum_{j=1}^3 p_{R_j}(n)$ .

Applying the above approximations, problem (12) can be solved by iteratively solving the convex problem (19), which is formulated for the  $n$ th iteration index as:

$$\max_{\mathbf{p}, z_i, x_i} \quad \sum_{i=1}^6 \log_2(1 + x_i) \quad (19a)$$

$$\text{s.t.} \quad p_{S_2} G_{S_2,R} + \theta p_B G_{B,R} + I_{R_L}(n) + \sigma_N^2 - z_1 \leq 0, \quad (19b)$$

$$\theta p_{S_1} G_{S_1,R} + \theta p_B G_{B,R} + I_{R_L}(n) + \sigma_N^2 - z_2 \leq 0, \quad (19c)$$

$$p_{S_1} G_{S_1,R} + p_{S_2} G_{S_2,R} + I_{R_L}(n) + \sigma_N^2 - z_3 \leq 0, \quad (19d)$$

$$\theta G_{R,B} \sum_{j=1,2} p_{R_j} + \sum_{k=1,2} p_{S_k} G_{S_k,B} + I_{B_L}(n)$$

$$+ \sigma_N^2 - z_6 \leq 0, \quad (19e)$$

$$h_q(\mathbf{p}) - z_q \leq 0 \quad \forall q = [4, 5], \quad (19f)$$

$$\frac{1}{2\hat{\xi}_i(n)} x_i^2 + \frac{\hat{\xi}_i(n)}{2} z_i^2 - g_i(\mathbf{p}) \leq 0 \quad \forall i, \quad (19g)$$

$$(12b) - (12f). \quad (19h)$$

---

**Algorithm 1** Iterative Sum Rate Maximization Algorithm
 

---

**Input**  $\bar{p}_{S_1}, \bar{p}_{S_2}, \bar{p}_B, \bar{p}_R, G, \lambda, \theta, \sigma^2, C_{\min}$ , and tolerance ( $\epsilon$ ),

**Output**  $\mathbf{p}$  and  $C_{\text{tot}}$ ,

Set  $n := 0$  and initialize  $\mathbf{p}(n), z_i(n), x_i(n)$ , and  $\hat{\xi}_i(n)$  by  $\frac{x_i(n)}{z_i(n)}$ ,

1: **Repeat:**

2: Solve (19) for  $\mathbf{p}^*, z_i^*, x_i^* \forall i$ ;

3: Set  $n := n + 1$ ;

4: Update  $x_i(n)$  by  $x_i^*, z_i(n)$  by  $z_i^*$  and  $\hat{\xi}_i(n)$  by  $\frac{x_i^*}{z_i^*} \forall i$ ;

5: **Until** convergence of sum rate with tolerance  $\epsilon$ .

---

Problem (19) needs to be solved iteratively and the pseudocode for the proposed sum rate optimization algorithm is summarized in Algorithm 1.  $C_{\text{tot}}$  is the total sum rate on all channels.  $G$  is a set that consists of all the channel gains,  $G_{B,R}, G_{S_1,R}, G_{S_2,R}, G_{R,B}, G_{R,RA_1}, G_{R,RA_2}$ . The problem at the  $n$ th iteration is convex and the optimal solution of this iteration is a feasible input point to the problem at the  $(n+1)$ th iteration. It can be shown that the algorithm generates non-decreasing objective function values at each iteration. Since the problem is bounded from above by the power constraints, the algorithm converges to some local optimal solution.

## V. RESULTS AND DISCUSSION

In this section, we study the performance of the system as obtained by using Algorithm 1. The optimization problem is solved centrally at the buoy, which is assumed to have perfect knowledge of the channel gains.  $\bar{p}_{S_1}$  and  $\bar{p}_{S_2}$  are set to 0 dBW, while  $\bar{p}_B$  and  $\bar{p}_R$  are set to 4.8 dBW [16], [17].  $f_0$  is 10 kHz and  $W$  is 5.5 kHz [12].  $\beta$  and  $\mu$  are 38 dB and 18 dB, respectively [7], [11]. The noise is calculated based on moderate wind speed of 10 m/s, a maximum shipping activity factor of 1 and perfect circuit efficiency of 1 [13], [18]. The minimum sum rate for each channel ( $C_{\min}$ ) is 2 kbps. The tolerance,  $\epsilon$ , is set to  $10^{-4}$ . The algorithm is implemented using CVX with SDPT3 as the internal solver [19], [20].

Fig. 2 convergence behavior of Algorithm 1. For  $\lambda = 0.8$  and  $\theta = 0.1$ , the algorithm is ran for four different initial values. It can be observed that for all four initial values the algorithm converges within two iterations.

In order to benchmark the effect of adding the relay and employing FD and NOMA, the performance of relay-aided (R) FD-NOMA, non-relay (NR) aided FD-NOMA and relay-aided half duplex orthogonal multiple access (R-HD-OMA)

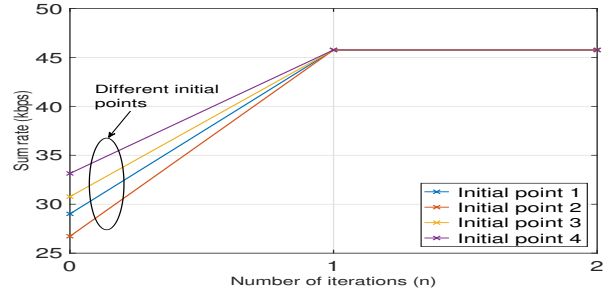


Fig. 2: The number of iterations to converge for SIC efficiency ( $\lambda$ ) = 0.8 at SuIC efficiency ( $\theta$ ) = 0.1.

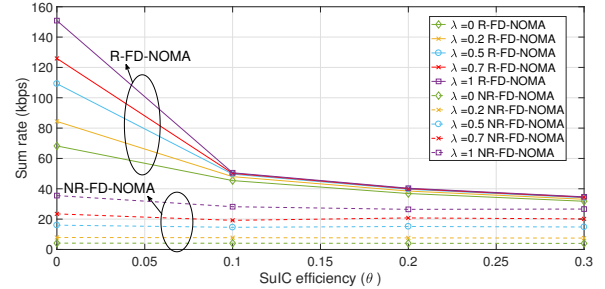


Fig. 3: Sum rate vs. SuIC efficiency ( $\theta$ ) at different SIC efficiencies.

are compared. In NR-FD-NOMA, it is assumed that there is no relay and hence the communication is direct between the buoy and the robotic arms or the sensors. The minimum guaranteed sum rate per channel is reduced to 0.8 kbps, due to the weak channels between the buoy and the seabed. The maximum power levels are kept the same. The other benchmark model is R-HD-OMA. In R-HD-OMA, it is assumed that each communication channel has a dedicated bandwidth. In addition, the bandwidth is divided equally among all concurrent transmissions. Only UL or DL communications can take place during one time slot. Consequently, for the UL and DL communications to take place, two time slots are needed. Each transmission utilizes different time or frequency resources and hence, there is no interference. The absence of interference between different transmissions means that the SIC and SuIC efficiencies will have no effect on the power or the sum rate of the system. The same constraints from (12) are applied to the transmission. For a fair comparison, the sum rate of two time slots will be considered. The channel conditions are assumed to be the same in both time slots. The results are depicted in Figs. 3-7.

Fig. 3 shows that as the efficiency of SuIC increases, represented as a decrease in  $\theta$ , the sum rate increases. As the SuIC efficiency increases, the interference from other transmissions due to NOMA decreases, and consequently the sum rate increases. It is assumed that if  $\theta > 0.3$ , the SuIC efficiency is not acceptable. Similarly, Fig. 3 shows that as the efficiency of SIC increases, represented as an increase in  $\lambda$ , the sum rate increases. This shows that as the isolation between

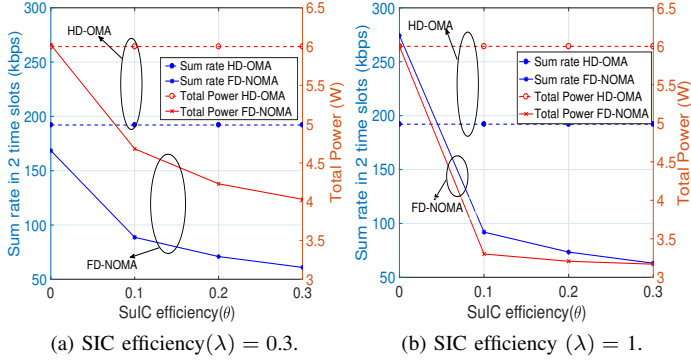


Fig. 4: Sum rate and total power vs. SuIC efficiency ( $\theta$ ) at different SIC efficiencies ( $\lambda$ ).

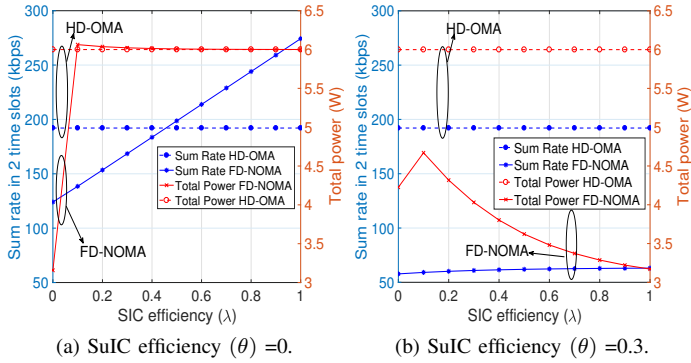


Fig. 5: Sum rate and total power vs. SIC efficiency ( $\lambda$ ) at different SuIC efficiencies ( $\theta$ ).

the DL and UL signals increases, interference decreases, and hence the sum rate increases. Maximum sum rate is achieved at  $\lambda = 1$  and  $\theta = 0$ , where the minimal interference occurs.

Fig. 3 also compares R-FD-NOMA and the NR-FD-NOMA. R-FD-NOMA always supports higher sum rate when compared to NR-FD-NOMA, irrespective of the SuIC and SIC efficiencies. It is shown that R-FD-NOMA can (at  $\theta = 0$  and  $\lambda = 0.2$ ) outperform the sum rate of the system when compared to the NR-FD-NOMA.

Figures 4-7 compare R-FD-NOMA with R-HD-OMA as per the total power consumed (shown on the right hand side y-axis) and the sum rate (shown on the left hand side y-axis). Total power refers to the sum of the power required by all devices. Note that the letter ‘‘R’’ is omitted in the figures for simplicity.

In R-HD-OMA, the absence of interference between different transmissions means that the SIC and SuIC efficiencies will have no effect on the power or the sum rate of the system. This is shown in Figs. 4 and 5, where the sum rate for the R-HD-OMA system is constant at 190 kbps and the total power consumed by all nodes is constant at 6 W for all  $\theta$  and  $\lambda$ . For a single time slot in R-FD-NOMA, all UL and DL transmissions are performed consuming the full bandwidth.

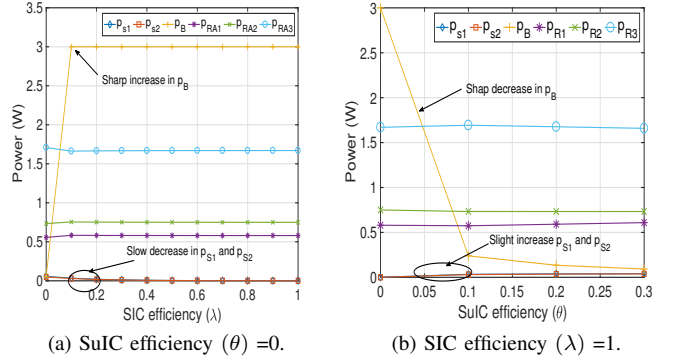


Fig. 6: Power vs. SIC efficiency ( $\lambda$ ) at ( $\theta$ ) = 0 and SuIC efficiency at ( $\lambda$ ) = 1.

As seen from Fig. 4, the SuIC has to be efficient for R-FD-NOMA to provide a higher sum rate than R-HD-OMA. The sum rate at a good SuIC can provide up to 30% increase in rate of R-FD-NOMA when compared to sum rate of R-HD-OMA. Also, the figure shows that as the efficiency increases ( $\theta$  decreases) more capacity could be achieved and hence more power is needed. Fig. 5 shows that at  $\theta = 0$ , if the SIC efficiency ( $\lambda$ ) is greater than 0.4, the sum rate of the R-FD-NOMA is greater than can the sum rate of the R-HD-OMA.

In order to further understand the behavior of the total power in Figs. 4 and 5, individual node powers are studied in Fig. 6. Given that the effect of the interference on each transmission is different, the transmission power on each channel is altered individually to cater for the highest possible total sum rate. In addition, the buoy has the highest possible power of all nodes, thus a sharp increase in  $p_B$  leads to an overall increase in the total power. In Fig. 5a, it is shown that the power increases once  $\lambda$  takes a non-zero value. Then, the power decreases slowly afterwards. From Fig. 6a, it can be seen that the main reason for the spike was an increase in the  $p_B$ . This increase is based on the nature of the RSI model in (1). At  $\lambda = 0$ , the SI is at its maximum as nearly no SIC mechanism is applied, and the term for RSI in (1) is reduced to  $p/\beta$ . Hence, the effect of the power on the RSI increased. Once  $\lambda$  takes a non-zero value, the original term for the RSI is operational. Given that  $\theta = 0$ , the power increase at the buoy does not cause interference due to NOMA. Consequently,  $p_B$  goes to its maximum level; hence, the total power of the system increases. At the same time, as  $\lambda$  increases, the power needed by  $S_1$  and  $S_2$  to combat the interference decreases. This is not reflected in Fig. 5a for  $0 \leq \lambda \leq 0.1$  due to the increase in  $p_B$ , but as  $p_B$  reaches its maximum, the effect of the decrease in  $p_{s_1}$  and  $p_{s_2}$  shows a slight decrease in the total power. The power at the relay exhibits similar performance as the buoy. Similarly, from Figs. 6b and 4b, when  $\lambda = 1$ , at  $\theta = 0$ , the buoy transmits at its maximum power. As  $\theta$  increases,  $p_B$  decreases to avoid causing interference on other NOMA links. While, for the sensors, as the efficiency decreases, the power increases in an attempt to combat the effect of the interference. However, the effect

from that slight increase is not reflected in Fig. 4b, because  $p_B$  continued to decrease at a higher rate than the increase in  $p_{S_1}$  and  $p_{S_2}$ .

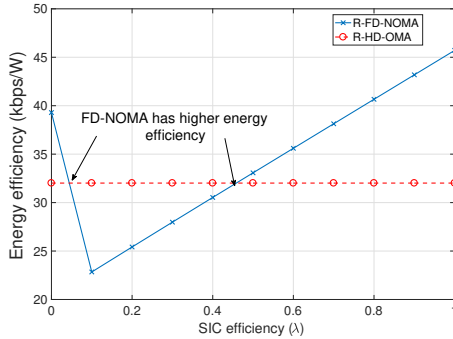


Fig. 7: Energy efficiency vs. SIC efficiency ( $\lambda$ ) at SuIC efficiency ( $\theta$ ) = 0.

In terms of power deficiency, at perfect SuIC with  $\lambda = 0$ , although the sum rate of R-FD-NOMA is lower than that of R-HD-OMA, R-FD-NOMA could be preferred because of higher energy efficiency as shown in Fig. 7.

## VI. CONCLUSION

In this paper, R-FD-NOMA UWA was investigated in order to increase the sum rate of the UWA channel without utilizing additional radio resources. The proposed optimization problem varies the power level at the network devices to provide the highest possible sum rate. Expressions for the sum rate of the R-FD-NOMA UWA system were derived and the sum rate maximization problem was formulated. As the problem is non-convex, a low-complexity iterative algorithm was proposed to obtain a sub-optimal-solution. The problem was solved centrally at buoy. Numerical simulations showed a direct relation between the sum rate and the interference cancellation efficiency and advocates for relay-aided communications. The results showed that R-FD-NOMA performs better than R-HD-OMA at high SuIC efficiency. Given a perfect SuIC, an increase in the efficiency of the SIC provides a higher sum rate at a better energy efficiency when compared to R-HD-OMA as long as  $\lambda$  is greater than or equal to 0.4. For lower values of  $\lambda$ , R-HD-OMA provides better sum rate than R-FD-NOMA. However, R-FD-NOMA could be preferred at low SIC efficiency, where it may provide higher energy efficiency.

## VII. ACKNOWLEDGMENT

The authors would like to acknowledge the support provided through the Research Chair in Subsea Communications, by Memorial University and Equinor.

## REFERENCES

[1] S. Jiang, "On reliable data transfer in underwater acoustic networks: A survey from networking perspective," *IEEE Commun. Surveys Tuts.*, 2018, doi: 10.1109/comst.2018.2793964.

[2] C. Gussen, P. Diniz, M. Campos, W. A. Martins, F. M. Costa, and J. N. Gois, "A survey of underwater wireless communication technologies," *J. Commun. Inf. Sys.*, vol. 31, no. 1, pp. 242–255, Oct. 2016.

[3] A. Gkikopouli, G. Nikolakopoulos, and S. Manesis, "A survey on underwater wireless sensor networks and applications," in *Proc. 20th IEEE Mediterranean Conf. on Control & Automation (MED)*, Jul. 2012, pp. 1147–1154.

[4] Y. Li, Y. Zhang, H. Zhou, and T. Jiang, "To relay or not to relay: Open distance and optimal deployment for linear underwater acoustic networks," to appear in *IEEE Trans. Commun.*, 2018, doi: 10.1109/tcomm.2018.2822287.

[5] A. Yadav and O. A. Dobre, "All technologies work together for good: A glance to future mobile networks," to appear in *IEEE Wireless Commun.*, 2018. [Online]. Available: arXiv preprint arXiv:1804.05963.

[6] S. R. Islam, N. Avazov, O. A. Dobre, and K.-S. Kwak, "Power-domain non-orthogonal multiple access (NOMA) in 5G systems: Potentials and challenges," *IEEE Commun. Surv. Tut.*, vol. 19, no. 2, pp. 721–742, Sept. 2017.

[7] M. Duarte, C. Dick, and A. Sabharwal, "Experiment-driven characterization of full-duplex wireless systems," *IEEE Trans. Wireless Commun.*, vol. 11, no. 12, pp. 4296–4307, Nov. 2012.

[8] M. F. Kader, S. Y. Shin, and V. C. Leung, "Full-duplex non-orthogonal multiple access in cooperative relay sharing for 5G systems," *IEEE Trans. Veh. Technol.*, 2018, doi: 10.1109/tvt.2018.2799939.

[9] F. Qu, H. Yang, G. Yu, and L. Yang, "In-band full-duplex communications for underwater acoustic networks," *IEEE Netw.*, vol. 31, no. 5, pp. 59–65, Sept. 2017.

[10] J. Cheon and H.-S. Cho, "Power allocation scheme for non-orthogonal multiple access in underwater acoustic communications," *Sensors*, vol. 17, no. 11, pp. 2465–2478, Oct. 2017.

[11] N. Shende, O. Gurbuz, and E. Erkip, "Half-duplex or full-duplex relaying: A capacity analysis under self-interference," in *Proc 47th IEEE Annu. Conf. Inf. Sci. Syst.*, 2013, pp. 1–6.

[12] P. Qarabaqi and M. Stojanovic, "Statistical characterization and computationally efficient modeling of a class of underwater acoustic communication channels," *IEEE J. Ocean. Eng.*, vol. 38, no. 4, pp. 701–717, Sept. 2013.

[13] R. F. Coates, *Underwater Acoustic Systems*. Macmillan International Higher Education, 1990, ch. 6, pp. 90–100.

[14] A. Yadav, O. A. Dobre, and N. Ansari, "Energy and traffic aware full-duplex communications for 5G systems," *IEEE Access*, vol. 5, pp. 11 278–11 290, May 2017.

[15] C. Canuto and A. Tabacco, *Taylor expansions and applications*. Milano: Springer Milan, 2008, ch. 7, pp. 223–255.

[16] Evologics, "Underwater acoustic communication system s2cr 7/17d product information," datasheet, Sep. 2016. [Online]. Available: <https://goo.gl/2SW6Qn>

[17] Evologics, "Usbl positioning and communication system s2cr 7/17 usbl product information," datasheet, Jun. 2012. [Online]. Available: <https://goo.gl/SMLFGE>

[18] M. Stojanovic, "On the relationship between capacity and distance in an underwater acoustic communication channel," *SIGMOBILE*, vol. 11, no. 4, pp. 34–43, Oct. 2007.

[19] M. Grant and S. Boyd, "CVX: Matlab software for disciplined convex programming, version 2.1," Mar. 2014. [Online]. Available: <http://cvxr.com/cvx>

[20] M. Grant and S. Boyd, "Graph implementations for nonsmooth convex programs," in *Recent Advances in Learning and Control*, ser. Lecture Notes in Control and Information Sciences, V. Blondel, S. Boyd, and H. Kimura, Eds. Springer-Verlag Limited, 2008, pp. 95–110.